Acta Cryst. (1990). B46, 267–275

A 'Concentration-Wave' Approach to Understanding the Disorder Diffuse Scattering in 1,3-Dibromo-2,5-diethyl-4,6-dimethylbenzene, $C_{12}H_{16}Br_2$

BY T. R. WELBERRY, R. L. WITHERS AND J. C. OSBORN

Research School of Chemistry, Australian National University, PO Box 4, Canberra City, ACT 2601, Australia

(*Received* 30 *October* 1989; *accepted* 20 *November* 1989)

Abstract

The origins of an unusual diffraction phenomenon which occurs in 1,3-dibromo-2,5-diethyl-4,6-dimethylbenzene are discussed. A distinct 'hole' is observed in the disorder diffuse scattering distribution at wavevectors close to $\mathbf{q} = 0$. If the diffuse intensity distribution is described in terms of concentration waves which modulate an *average* $P2_1/c$ structure, two different types of mode are possible, a Σ_1 mode which tends to preserve a 2_1-screw axis relationship between neighbouring molecules and a Σ_2 mode which tends to preserve a *c*-glide plane relationship. We show that the observed diffuse scattering is practically completely explained in terms of modulations which are of the Σ_2 symmetry, even though the determined *average* crystal structure (space group $P2_1$) corresponds to a frozen-in Σ_1 mode. We conclude that the short-range order, which tends locally to preserve the *c*-glide plane, is due to dipole–dipole interactions between molecules, while the stability of the lattice over a long range (corresponding to wavevectors close to $\mathbf{q} = 0$) results from the ability of the molecules to form a closely packed structure in three different crystallographic planes, and this is governed by the short-range repulsive interactions. The 'hole' represents a range of wavevectors for which the strain from the packing forces, resulting from the local breaking of the $P2_1$ symmetry, outweighs the energy gained from the short-range ordering of the molecular dipoles.

1. Introduction

In previous papers (Welberry & Jones, 1980; Epstein, Welberry & Jones, 1982; Epstein & Welberry, 1983; Welberry & Siripitayananon, 1986, 1987) we have described our interest in disordered molecular crystals. In particular we have described a number of examples in which disorder occurs because the disposition of methyl and bromo or chloro groups around an aromatic centre allows the molecule to take up either one of two different orientations in a given molecular site in the crystal with very little difference in energy. This possibility of disorder arises because of the similarity in size and shape of these constituent groups for crystal-packing purposes, and the large difference in X-ray scattering power between methyl and halogen makes these systems ideal examples for study of the resulting diffuse scattering distributions.

In the earliest studies the results obtained were barely more than qualitative descriptions of the short-range ordering effects but later studies were carried out at a more quantitative level as a result of improved methods of recording the diffuse scattering data, and the development of a method of analysing the scattering using a least-squares procedure to fit a model of the disorder to the observed intensities. These later diffuse scattering experiments yielded quantitative information concerning the mutual orientation of neighbouring molecules. Values were determined for the correlation coefficients, $C_{n,m}$, for all intermolecular vectors within a given neighbourhood of a particular molecule. Here $C_{n,m} = (P_{AA} - m_A^2)/m_A m_B$, where P_{AA} is the joint probability that both sites n and m are occupied by molecules of the same type (orientation) A, and m_A and m_B are site occupancies. The analysis uses so-called *random* and *correlation-distribution* functions as basis functions for the least-squares procedure which establishes the values of the $C_{n,m}$ giving the best fit to the observed data. Further details of the procedure can be found in Epstein & Welberry (1983) and Welberry & Siripitayananon (1986).

While the early qualitative results seemed to indicate that a simple model of interacting molecular dipoles might account for the short-range order observed, the most recent studies on the system of substituted *p*-diethylbenzenes indicated that such a simplistic view was unsatisfactory. Of particular note was the fact that the diffraction patterns of 1,3-dibromo-2,5-diethyl-4,6-dimethylbenzene (BEMB2 – see Fig. 1, Table 1) contained some striking features which were not satisfactorily accounted for by the short-range correlations. These effects are best seen in the $(0kl)$ and $(hk\bar{h})$ reciprocal sections which we show in Fig. 2. The patterns show strong diffuse

0108-7681/90/020267-09$03.00

bands of intensity extending in the **b*** direction, which may be seen around the (010) and (002) reciprocal positions in the (0*kl*) section, and around (010) in the (*hkl̄*) section. Note that the (*hkl̄*) section is approximately normal to the (0*kl*) section. In (0*kl*) the diffuse bands are generally quite broad, consistent with the small values of the nearest-neighbour correlation coefficients obtained from the least-squares fitting, but there is a distinct narrowing of the band close to (010) or (002) with the width at this point being indicative of a range of order along **c*** far exceeding that suggested by the short-range correlations. In the (*hkh*) section this same feature is seen as a 'hole' in the diffuse scattering around the (010) reciprocal position. Attention was drawn to this very unusual diffraction feature in Welberry & Siripitayananon (1987), but no suitable explanation was put forward at that time.

In this paper we present the results of further investigations into this phenomenon. Instead of using a correlation or short-range-order parameter description of disorder, commonly used for example in studies of alloys (*e.g.* Hawakawa, Bardhan & Cohen, 1975; Cenedese, Bley & Lefebvre, 1984), we make use of an alternative description of the disorder involving the concept of 'concentration waves'. Such concepts have been used, for example, by de Fontaine (1972, 1973) and more recently have been widely used to describe incommensurately modulated structures (McConnell & Heine, 1985; Yamamoto, 1982; Withers, Thompson & Hyde, 1989) for which a short-range-order description would seem inappropriate.

2. Concentration waves

The diffuse intensity occurring at any point in reciprocal space defined by the wavevector $\mathbf{G}+\mathbf{q}$, where $\mathbf{G}$ is a reciprocal lattice vector and $\mathbf{q}$ is a vector within the first Brillouin zone, can be considered to arise from a periodic perturbation of the real-space structure. For the case of concentration waves these perturbations can be written in the form of a variation from cell to cell of the atomic scattering factors f_μ, where μ specifies an atomic site within the average unit cell. It is convenient to describe the perturbations in terms of variations about the mean values and we write,

$$f_\mu(\mathbf{T}) = \langle f_\mu\rangle + \delta f_\mu(\mathbf{T})$$

where,

$$\delta f_\mu(\mathbf{T}) = \langle f_\mu\rangle\{\sum_q 2A_\mu(\mathbf{q})\cos[2\pi\mathbf{q}.\mathbf{T} + \theta_\mu(\mathbf{q})]\} \quad (1)$$

and $\mathbf{T}$ is a vector defining the position of each unit cell. Putting $A_\mu\exp(i\theta_\mu) = a_\mu$, we obtain

$$f_\mu(\mathbf{T}) = \langle f_\mu\rangle\{1 + \sum_q[a_\mu(\mathbf{q})\exp(2\pi i\mathbf{q}.\mathbf{T}) + a^*_\mu(\mathbf{q})\exp(-2\pi i\mathbf{q}.\mathbf{T})]\}. \quad (2)$$

To obtain the structure factor $F(\mathbf{k})$ we use

$$F(\mathbf{k}) = \sum_r f_\mu\exp\{-2\pi i\mathbf{k}.\mathbf{r}\} = \sum_\mu\sum_T f_\mu(\mathbf{T})\exp\{-2\pi i\mathbf{k}.\mathbf{r}_\mu\}\exp\{-2\pi i\mathbf{k}.\mathbf{T}\} \quad (3)$$

where $\mathbf{r} = \mathbf{r}_\mu + \mathbf{T}.\mathbf{r}_\mu$ defines the position of the μth atom within the unit cell and $\mathbf{T}$ defines the real-space lattice vectors. From (3) we can obtain,

$$F(\mathbf{G}+\mathbf{q}) = \sum_\mu\langle f_\mu\rangle a_\mu\exp\{-2\pi i(\mathbf{G}+\mathbf{q}).\mathbf{r}_\mu\}. \quad (4)$$

Equation (4) indicates that the amplitude of the scattering at a point $\mathbf{G}+\mathbf{q}$ in reciprocal space is directly proportional to the amplitude in real space of the modulation having the wavevector $\mathbf{q}$.

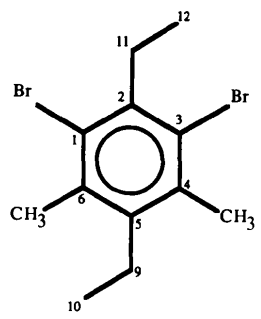

Fig. 1. The BEMB2 molecule showing the atomic numbering referred to in Table 1.

Table 1. *Cell data and atomic coordinates of BEMB2 [after Wood et al. (1984) – note change of origin]*

The fractional coordinates (x, y, z) listed below refer to a molecule in site 1. The coordinates for a molecule in site 2 are obtained as ($-x$, $y+0.5$, $0.5-z$).

Space group: $P2_1$
Cell dimensions: $a = 9.086$, $b = 4.442$, $c = 17.969$ Å, $\beta = 122.69°$

	Molecular orientation 1			Molecular orientation 2		
	x	y	z	x	y	z
Br[C(1)]	0.2806	0.2371	−0.0469	0.4125	−0.1191	0.1321
Br[C(3)]	−0.4134	0.1147	−0.1310	−0.2819	−0.2638	0.0456
C[C(4)]	−0.2327	−0.2504	0.0452	−0.3704	0.1360	−0.1162
C[C(6)]	0.3697	−0.1409	0.1170	0.2345	0.2587	−0.0397
C(1)	0.1094	0.1073	−0.0289	0.1735	−0.0640	0.0645
C(2)	−0.0712	0.1554	−0.0819	0.0471	−0.1745	0.0791
C(3)	−0.1781	0.0351	−0.0554	−0.1286	−0.1043	0.0187
C(4)	−0.1047	−0.1305	0.0229	−0.1763	0.0739	−0.0551
C(5)	0.0754	−0.1799	0.0762	−0.0512	0.1855	−0.0703
C(6)	0.1811	−0.0591	0.0493	0.1238	0.1143	−0.0097
C(7)	−0.1321	0.3398	−0.1651	0.1185	−0.3653	0.1622
C(8)	−0.1668	0.1325	−0.2417	0.1796	−0.1870	0.2476
C(9)	0.1360	−0.3640	0.1593	−0.1227	0.3758	−0.1532
C(10)	0.1775	−0.1999	0.2393	−0.1671	0.1795	−0.2334

3. Symmetry considerations

3.1. $\mathbf{q} = 0$ *modulations*

Modulations of the form (2) must be consistent with the space-group symmetry of the average structure, and this imposes restrictions on the allowed values for a_μ for modulations with wavevectors along certain symmetry directions. In the following description we use the nomenclature of Bradley & Cracknell (1972). In this notation a symmetry element is written in the form of an operator $\{R|\mathbf{v}\}$ where $\mathbf{v}$ is a vector translation associated with the symmetry operator R. Thus for example in Fig. 3(*c*), which shows the average structure of BEMB2, the molecule at $\mathbf{b} = 0$, $\mathbf{c} = 0$ is related by a 2_1 screw (C_{2y}) to the one at $\mathbf{b} = 0{\cdot}5$, $\mathbf{c} = 0{\cdot}5$ by the operator $\{C_{2y}|(\mathbf{b} + \mathbf{c})/2\}$.

The average structure of BEMB2 conforms to the space group $P2_1$, but in fact is very close to $P2_1/c$. In

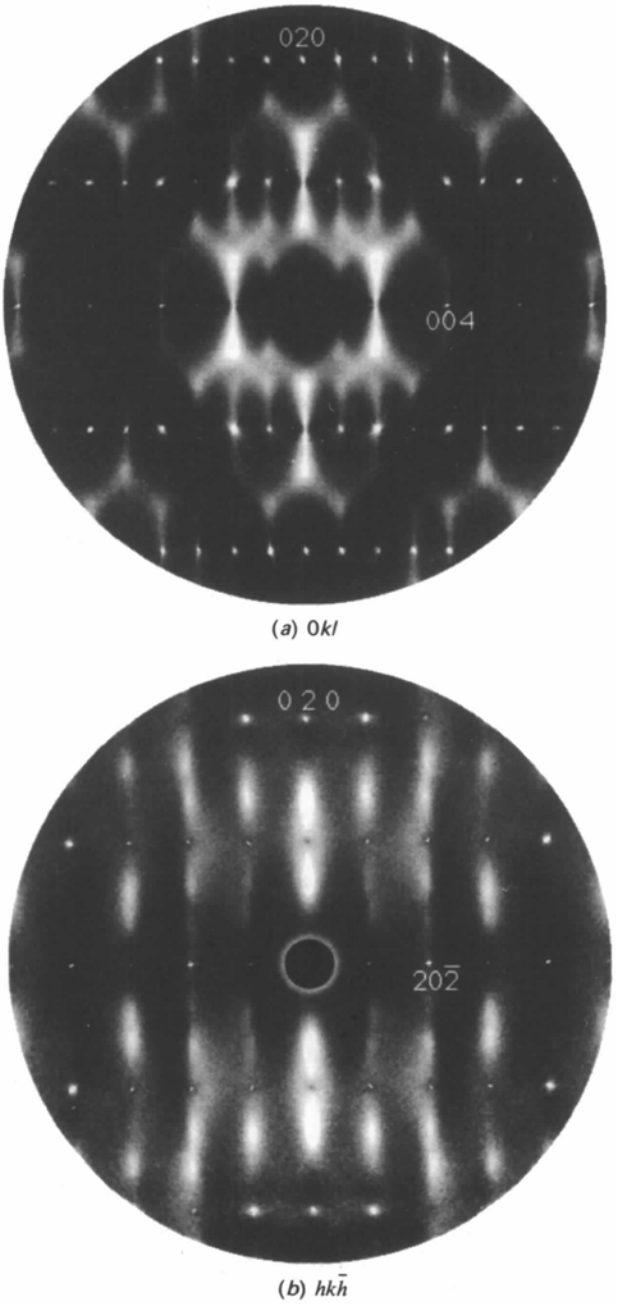

Fig. 2. X-ray diffraction patterns at 120 K of BEMB2. (*a*) The 0*kl* section. (*b*) The *hk*$\bar{h}$ section. The outer perimeter of the patterns corresponds to a diffraction angle $\theta_{\mathrm{Cu}\ K\alpha} = 25{\cdot}6°$.

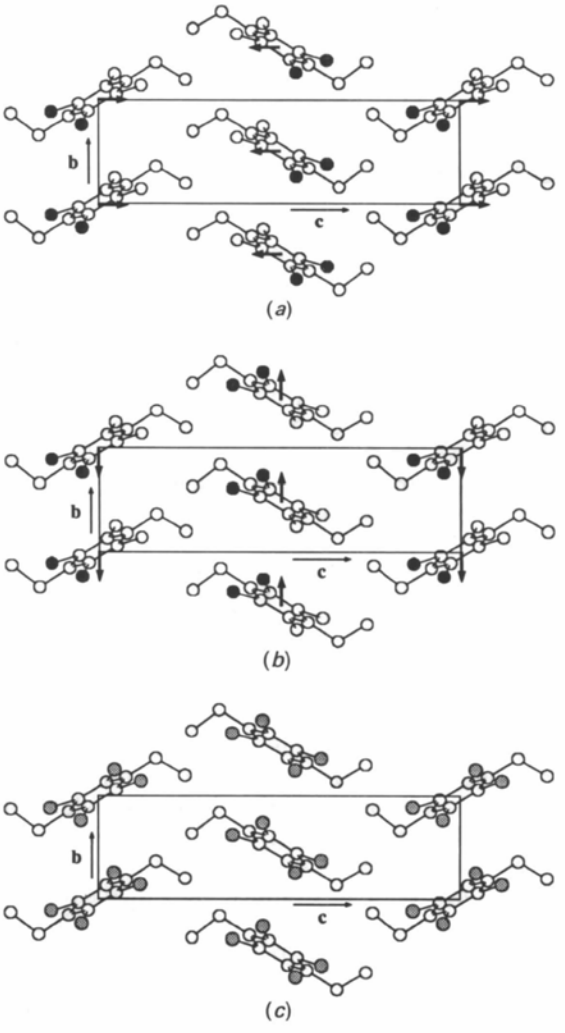

Fig. 3. The structure of BEMB2 projected down the *a* axis. (*a*) The structure in which the 2_1-screw symmetry is satisfied (the Σ_1 mode). (*b*) The structure in which the *c*-glide symmetry is satisfied (the Σ_2 mode). (*c*) Represents the *average* structure as revealed by analysis of the Bragg diffraction data which approximately satisfies both the 2_1-screw and the *c*-glide symmetry. Black circles represent Br atoms and open circles C atoms. The shaded circles in (*c*) represent a composite Br/C disordered atom.

Fig. 3(*c*) the shaded substituent sites have a composition approximately ($0{\cdot}5Br + 0{\cdot}5CH_3$). Only a small number of weak Bragg peaks of the type (*h*0*l*), with *l* odd, reveal the breaking of the *c*-glide symmetry. The structure can therefore be considered as a $P2_1/c$ structure containing a weak $\mathbf{q} = 0$ modulation which destroys the *c* glide but maintains the 2_1-screw axis.

The isogonal point group of $P2_1/c = F = \{E, i, C_{2y}, \sigma_y\}$, and the little co-group of the modulation wavevector $\mathbf{q} = 0$, *i.e.* the sub-group of *F* which maps $\mathbf{q}$ into itself is also $\{E, i, C_{2y}, \sigma_y\}$. The corresponding table of irreducible representations is given by:

	E	i	C_{2y}	σ_y
Γ_1	1	1	1	1
Γ_2	1	1	−1	−1
Γ_3	1	−1	1	−1
Γ_4	1	−1	−1	1

In general we can write,

$$\{R|\mathbf{v}\}\begin{Bmatrix}\delta f_\mu(\mathbf{T})\\ \mathbf{u}_\mu(\mathbf{T})\end{Bmatrix} \rightarrow \begin{Bmatrix}\delta f_\mu(\mathbf{T})\\ \mathbf{u}_\mu(\mathbf{T})\end{Bmatrix}\chi^j(R)\exp(-2\pi i\mathbf{q}.\mathbf{v}) \tag{5}$$

where $\chi^j(R)$ is the character given in the above table, $\delta f_\mu(\mathbf{T})$ describes a compositional modulation of the parent structure as given by (1) and (2), and $\mathbf{u}_\mu(\mathbf{T})$ similarly a displacive modulation (which for the present we shall ignore), characterized by the modulation wavevector $\mathbf{q}$ and for which $R\mathbf{q} \equiv \mathbf{q}$. In our case $\mathbf{q} = 0$ and consequently,

$$\{R|\mathbf{v}\}\begin{Bmatrix}\delta f_\mu(\mathbf{T})\\ \mathbf{u}_\mu(\mathbf{T})\end{Bmatrix} \rightarrow \begin{Bmatrix}\delta f_\mu(\mathbf{T})\\ \mathbf{u}_\mu(\mathbf{T})\end{Bmatrix}\chi^j(R). \tag{6}$$

A character of +1 under a particular symmetry operation *R* in the above table thus implies that the corresponding space-group symmetry operation $\{R|\mathbf{v}\}$ is preserved in the resultant structure. Thus a modulation which has a character of 1 in the third column of Table 1 will preserve the 2_1 screw, while one having a character of 1 in the fourth column will preserve the *c*-glide plane. It is clear that for compositional modulations in which individual sites must contain the non-centrosymmetric BEMB2 molecule in one or other of its two possible orientations, a modulation of Γ_1 or Γ_2 symmetry is not possible, since these require that the four substituent sites in one molecular site maintain the same composition. A modulation of Γ_3 symmetry (for which the eigenvector is $a_1 = 1$, $a_2 = 1$) is possible, however, and produces a structure with the appearance of Fig. 3(*a*), which preserves the 2_1-screw axis. A modulation of Γ_4 symmetry (for which the eigenvector is $a_1 = 1$, $a_2 = -1$) is also possible and produces a structure with the appearance of Fig. 3(*b*). This destroys the 2_1-screw axis and preserves the *c*-glide symmetry. It is clear from experiment that the departure of the average structure from the idealized $P2_1/c$ structure must be describable in terms of a $\mathbf{q} = 0$, Γ_3 modulation. It should be stressed here that since we are talking about a $\mathbf{q} = 0$ modulation the differences from the idealized $P2_1/c$ structure occur on average over the whole crystal. This means in effect that the occupancies of the two molecular sites within the average unit cell are different from 0·5 [the actual crystal structure refinement yielded values which differed from 0·5 only in the third decimal place (Wood, Welberry & Puza, 1984)]. Fig. 3(*a*) can be taken as representing the average crystal structure, in this case, if the black circles are taken to represent substituent sites containing slightly more than 0·5Br and the white substituent sites correspondingly slightly less than 0·5Br. While these differences from 0·5 are small, the fact that they exist is *highly* significant and we will return to this point later.

3.2. $\boldsymbol{q} \neq 0$ *modulations*

For a general wavevector $\mathbf{q}$ there are no symmetry restrictions constraining the choice of the two permissible types of concentration modulation Γ_3 or Γ_4, and in general the lowest energy modulation at a particular $\mathbf{q}$ might be expected to be a linear combination of the two. The eigenvector (a_1, a_2) defining this mixture depends on the energy of the system and not on the symmetry. Most of the observed diffuse intensity occurs close to $\mathbf{G} \pm q\mathbf{b}^*$ where $0 < q < \sim 0{\cdot}4$. For modulation wavevectors along $\mathbf{b}^*$, the little co-group = $\{E, C_{2y}\}$. Here there are two corresponding irreducible representations:

	E	C_{2y}
Σ_1	1	1
Σ_2	1	−1

Since molecular sites 1 and 2 within the average unit cell are related by the 2_1-screw (C_{2y}) axis, (5) leads to the requirements that,

$$a_2 = \pm a_1\exp[2\pi i\mathbf{q}.(\mathbf{b} + \mathbf{c})/2] \tag{7}$$

where the + sign corresponds to a Σ_1 mode and the − sign to a Σ_2 mode. Clearly Σ_1 and Σ_2 merge with Γ_3 and Γ_4, respectively, at the origin of reciprocal space.

4. Computer simulation and optical transforms

It is interesting to compare the effects of the two different types of modulation, described in the last section, on the diffuse scattering distribution. To do this we make use of computer-simulation and optical-transform techniques (Lipson, 1973, Harburn, Miller & Welberry, 1974; Harburn, Taylor &

Welberry, 1975). We have previously described a method for synthesizing a real-space distribution of scattering points which will give rise to a predetermined diffuse scattering distribution (Welberry & Withers, 1987), and this has recently been extended to allow the possibility of multiple disordered sites within a unit cell (Welberry & Withers, 1990). The method essentially consists of constructing in the computer a lattice of random variables which are subject to a large number of perturbing modulations whose amplitudes are chosen to match the intensity distribution in the first Brillouin zone of the observed pattern. The final array of random variables is used to construct an actual lattice realization using the atomic coordinates of the two different molecular orientations derived from the average crystal structure determination.

In the first Brillouin zone of the (0*kl*) section of BEMB2 (Fig. 2*a*) the diffuse intensity distribution is seen to be in the shape of a 'Y' – the intense vertical

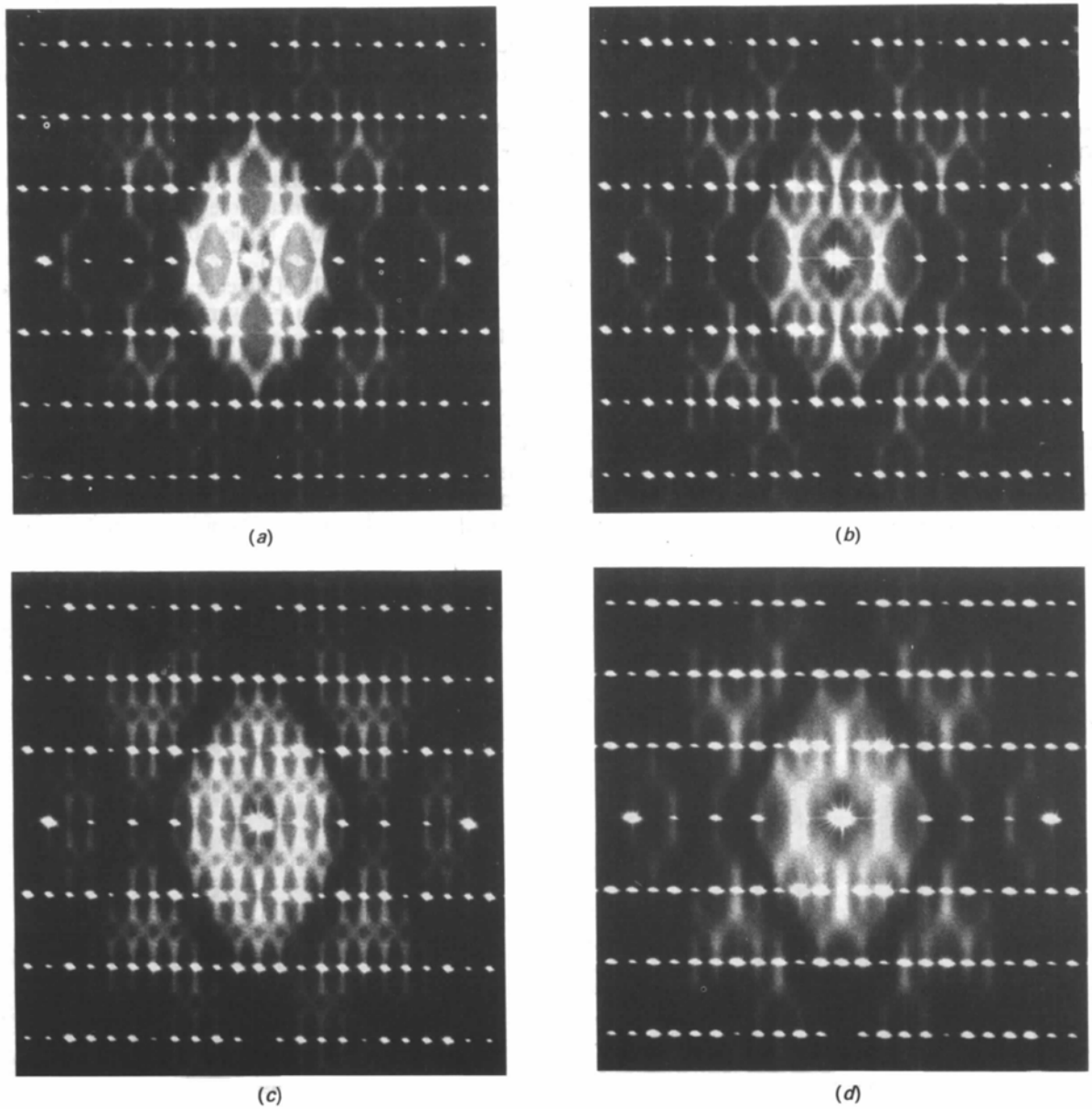

Fig. 4. Optical diffraction patterns of masks constructed using modulation-wave amplitudes which qualitatively matched the diffuse intensity distribution in the first Brillouin zone of the X-ray pattern of Fig. 2(*a*). In (*a*) only modulations of the Σ_1 symmetry are included; in (*b*) only modulations of the Σ_2 symmetry are included; and in (*c*) modulations which are an equal mixture of Σ_1 and Σ_2 are used. (*d*) Shows the pattern obtained from a mask derived from a simple model of interacting dipoles (see text).

part of the 'Y' extending along **b*** then splitting into the two weaker arms which end on the zone boundary at ($0{\cdot}5\mathbf{b}^* + 0{\cdot}5\mathbf{c}^*$). Optical diffraction masks were constructed using modulation-wave amplitudes which qualitatively matched this diffuse intensity distribution, and the optical transforms of these masks are shown in Fig. 4. In Fig. 4(*a*) only modulations of the Σ_1 symmetry were included; in Fig. 4(*b*) only modulations of the Σ_2 symmetry were included; and in Fig. 4(*c*) modulations which were an equal mixture of Σ_1 and Σ_2 were used.

It is clear from these pictures that Fig. 4(*b*) corresponds very closely to the observed X-ray diffuse scattering in BEMB2, while in Fig. 4(*a*) the intensity appears in all the wrong places, and Fig. 4(*c*) has intensity in both the right and wrong places. This means that the $\mathbf{q} \neq 0$ modulations of the structure are virtually entirely of Σ_2 symmetry. To be more specific, it can be seen that the Σ_2 modulations result in the strong 'Y' of scattering appearing around the (010), (002), (004), (008) Bragg positions, while for the Σ_1 modulations the scattering appears around the (020), (001), (003), (005) *etc.* peaks. It is clear from the experimental data that no trace can be seen of the band of diffuse scattering around (020), (001) or (003). *We therefore have the paradoxical situation that the compositional modulations of the structure for all wavevectors other than* $\mathbf{q} = 0$ *are of* Σ_2 *symmetry (which tends to preserve the c-glide plane and destroy the* 2_1*-screw axis), but for* $\mathbf{q} = 0$ *the modulation preserves the* 2_1*-screw axis and destroys the c glide; i. e. it has* Σ_1 *symmetry.*

The 'hole' in the diffuse scattering which is seen clearly in the ($hk\bar{h}$) section shown in Fig. 2 is evidently a manifestation of this incompatibility between what the short-range and long-range forces are attempting to do to the structure. The diffuse scattering is explained in terms of short-range forces that favour modulations which preserve the *c*-glide symmetry, but for wavevectors close to $\mathbf{q} = 0$, corresponding to large distances in real space, such modulations are energetically unfavourable because over a long range the structure prefers to maintain the screw axis.

In Fig. 5(*a*) we show the result of the synthesis of an optical diffraction screen representing the ($hk\bar{h}$) section. This was again constructed using only modulations having Σ_2 symmetry, with amplitudes chosen to match qualitatively the intensity in the X-ray pattern. In the diffraction pattern the scattering is seen to contain a diffuse band of intensity along the **b*** axis, tending to a maximum around **b***/3, but with a distinct 'hole' at wavevectors close to ($\mathbf{q} = 0$), particularly noticeable around the (010) reciprocal lattice position. for comparison we show in Fig. 5(*b*) the result of a second synthesis in which wavevectors close to $\mathbf{q} = 0$ were included.

It was found in constructing these diffraction screens that some of the details of the pattern were quite sensitive to the atomic coordinates used. For example, the way in which diffuse peaks are observed at $\frac{4}{3}\mathbf{b}^*$ for $h = 0$, 1, 2 and $\frac{5}{3}\mathbf{b}^*$ for $h = 2$, 3 in the X-ray pattern of Fig. 2(*b*) (which is approximately but not exactly reproduced in the optical pattern) is critically dependent on the Br coordinates, as similarly is the

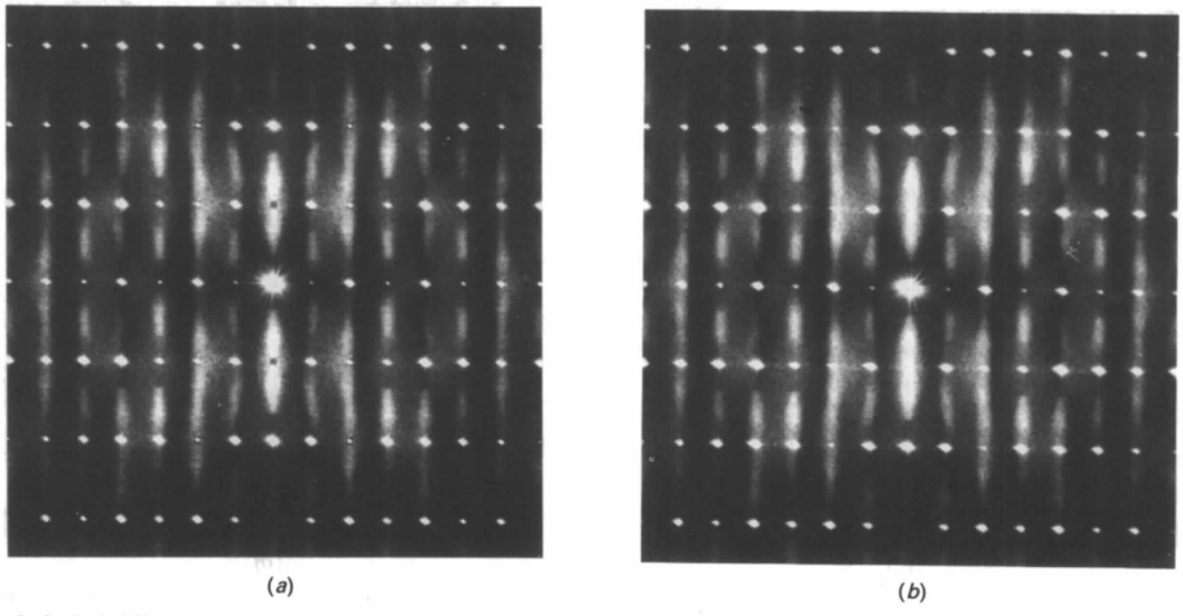

(*a*) (*b*)

Fig. 5. Optical diffraction patterns of masks constructed using modulation-wave amplitudes which qualitatively matched the diffuse intensity distribution in the first Brillouin zone of the X-ray pattern of Fig. 2(*b*). For (*a*) wavevectors close to $\mathbf{q} = 0$ were omitted from the synthesis while for (*b*) they were included.

absence of intensity along the $h = 4$ reciprocal row. The patterns shown were obtained using the coordinates obtained from the room-temperature average crystal structure, but in forming the optical diffraction screen these coordinates were approximated to the nearest plotting increment, which in some cases lead to a positional error of ~5%.

Since the synthesis leads to real-space lattice realizations, it is possible by summation over the lattice to obtain estimates of the intermolecular correlation coefficients, $C_{n,m}$, corresponding to these patterns, and it is interesting to compare those for the pattern with the 'hole' with those for the pattern without the 'hole' (see Table 2). It is seen from Table 2 that the actual numerical values differ only slightly in the two realizations, and it is clear than an analysis of the diffuse pattern in terms of correlation coefficients, as previously carried out by Welberry & Siripitayananon (1987) could not be expected to distinguish between the two, even if $C_{n,m}$ of sufficient spatial resolution were employed, since the experimental errors on the $C_{n,m}$ would be comparable to the small differences seen in Table 2. In reality the correlation field of the realization with the 'hole' has, superimposed upon the $C_{n,m}$ values, a low-level ripple which is the Fourier transform of the 'hole'. In the absence of statistical noise this can be seen in the higher-order $C_{n,m}$ values as they alternate between being slightly positive and slightly negative in concentric rings. For realizations of the size used in the present work, consisting of 512 × 512 lattice points, the statistical noise tends to mask this effect for the small size of hole used; but in examples in which a larger 'hole' was employed the effect could be seen quite clearly.

Table 2. *Correlation coefficients, $C_{n,m}$, for the synthesized lattice distribution used to obtain the optical diffraction pattern in Fig.* 5(*a*)

The figures in parentheses are the differences in the second place of decimals of this set of $C_{n,m}$ from those obtained from the lattice distribution used to obtain Fig. 5(*b*). The statistical counting error on each value is ~0·003.

	0·00 (1)							
		0·01 (−1)		0·01 (0)				
	−0·01 (1)		−0·01 (1)		−0·01 (0)			
		−0·02 (−1)		−0·01 (−1)		−0·01 (−2)		
	0·03 (2)		0·02 (2)		0·01 (2)			
		−0·02 (−2)		−0·01 (−2)		−0·01 (−2)		
	0·00 (1)		−0·01 (2)		0·00 (0)		0·01 (0)	
		0·11 (−3)		0·08 (−1)		0·03 (−1)		
	−0·03 (2)		−0·09 (2)		−0·06 (1)		−0·03 (0)	
↑		−0·29 (−1)		−0·13 (0)		−0·04 (0)		
[010]	1·0		0·41 (0)		0·20 (0)		0·07 (0)	[10$\bar{1}$]→
		−0·29 (−2)		−0·14 (−2)		−0·04 (−1)		
	−0·03 (2)		−0·09 (2)		−0·06 (2)		−0·04 (1)	
		0·11 (−2)		0·08 (−2)		0·04 (−1)		
	0·00 (1)		−0·01 (2)		0·00 (2)		0·00 (0)	
		−0·02 (−2)		−0·01 (−2)		0·00 (−1)		
	0·03 (2)		0·01 (2)		0·00 (1)			
		−0·01 (−1)		−0·01 (−1)		0·00 (−1)		
	−0·01 (1)		−0·01 (1)		−0·01 (1)			
		0·01 (−1)		0·01 (−1)				
	0·00 (1)							

5. Dipole–dipole interactions as the origin of short-range order

In order to demonstrate that diffuse scattering patterns having the general appearance of those observed in BEMB2 (but not including the long-range effects discussed above) can arise from interactions between molecular dipole moments, we decided to carry out a Monte-Carlo simulation of a simple two-dimensional model corresponding to the **a**-axis projection of structure shown in Fig. 3. We have previously used Monte-Carlo simulation in conjunction with optical transform techniques to investigate aspects of disorder in a number of different systems (Welberry, 1982, 1986; Welberry & Zemb, 1988; Hua, Welberry & Withers, 1988, 1989). In the present case, each molecule was represented by a simple dipole placed at the molecular centre and orientated along a vector joining the C(2) and C(5) atoms (*i.e.* parallel to the two bromine–methyl vectors). An array of 256 × 256 unit cells was used in order to have a sufficiently large sample to allow high-quality optical diffraction patterns to be obtained. A molecular dipole moment of 3 debye [estimated by comparison with other methyl, halogen-substituted benzenes – see *CRC Handbook of Chemistry and Physics* (Weast, 1988)] was assumed, and simulations were carried out for a number of different temperatures. At each step in the iteration procedure the relative energy of the two possible orientations of a dipole selected at random was computed (see *e.g.* Kitaigorodsky, 1973), and a decision made which orientation to choose using the usual Monte-Carlo criterion (Metropolis, Rosenbluth, Rosenbluth, Teller & Teller, 1953). A large number of cycles of iteration (> 200) were used in each case to ensure equilibrium was attained. Progress was monitored by computing lattice averages after each cycle. A cycle is defined as the number of individual steps required for each dipole to be visited once on average. Final configurations were then used to generate diffraction masks representing the actual BEMB2 molecules.

We show in Fig. 4(*d*) a diffraction pattern obtained from one simulation example, which corresponds to a temperature of 163 K. This example was chosen for illustration because the diffuseness of the scattering was comparable to that of the synthesized patterns of Figs. 4(*a–c*). Lower temperatures resulted in more sharply peaked, and higher temperatures more diffuse, distributions. No particular importance is attached to the actual magnitude of the temperature parameter for this rather crude two-dimensional model. The lattice averages computed for this example showed that the orientations of the molecules at the origin and the centre of the unit cell are

negatively correlated (with a correlation coefficient of $-0{\cdot}31$). A positive correlation would mean that there is a tendency for these neighbouring molecules to be related by the 2_1 screw and a negative correlation would mean a tendency towards the *c*-glide configuration. By contrast the orientations of molecules separated by one **c**-axis cell translation were positively correlated (with a coefficient of 0·21). What is of particular interest, is the fact that the pattern of correlations resulting from this rather simplistic model, reproduces the characteristic 'Y'-shaped diffuse distribution that is found in the X-ray patterns. There is, however, no tendency for the pattern to become particularly narrow at the $\mathbf{q} = 0$ positions.

It is qualitatively easy to see by comparing Figs. 3(*a*) and 3(*b*) that the configuration of dipoles corresponding to Fig. 3(*b*) will be more stable (as far as dipole–dipole interactions are concerned) than that for 3(*a*), since in 3(*b*) the dipoles are arranged essentially head-to-tail whereas in 3(*a*) they are essentially head-to-head. In fact if the dipole–dipole lattice sum (see *e.g.* Kitaigorodsky, 1973) is plotted as a function of the molecular orientation (tilt of the dipole away from the **b** axis say, while maintaining the lattice symmetry), the *c*-glide configuration in Fig. 3(*b*) is more stable than the 2_1-screw configuration for *any* degree of tilt. The actual observed tilts of the molecules are dictated by the very short-range repulsive potentials between atoms, and it is estimated (see Kitaigorodsky, 1973, p. 154) that additional dipole energies (because they are slowly varying functions of angle) cannot affect the tilt by more than about 1°.

6. Discussion

Kitaigorodsky (1973, and references therein) has discussed the ability of molecules to form closely packed structures in different space groups, and concludes that the predominance of the space group $P2_1/c$ for organic crystals occurs because only in this space group can closest-packed layers be built on all three coordinate planes of the unit cell simultaneously. He also concludes that the space group $P2_1$ is also among the next closest packed and is logically to be found in cases where the molecules do not have a centre of symmetry. It is clear, therefore, that a structure consisting of idealized *averaged* BEMB2 molecules would be $P2_1/c$ and a perfectly ordered structure of real BEMB2 molecules would be $P2_1$ if only packing considerations were important.

Locally in BEMB2, however, the dipole–dipole interactions override the long-range lattice stability, and molecules tend to assume orientations in which the *c*-glide symmetry rather than the 2_1 symmetry is satisfied locally. Though reducing the dipole–dipole contribution to the free energy, such a tendency must also result in a strain energy. It would be expected that this strain would be cumulative (*i.e.* the greater the range over which the *c* glide rather than the 2_1 symmetry is maintained, the greater the strain), so that eventually, at long range, it would become dominant and nullify the dipole–dipole interaction's preference to form the *c*-glide configuration.

It is frequently found in modulated structures that a concentration modulation of a certain symmetry is accompanied by a displacive modulation [see equation (5)] of the same symmetry (Toman & Frueh, 1976; Yamamoto, 1982). In Fig. 3 we have indicated by means of the arrows at the molecular centres the displacement patterns corresponding to $\mathbf{q} = 0$ phonons for the two types of mode depicted. It is clear that Σ_1 modes involve displacements in the **ac** plane, while Σ_2 modes involve displacements along **b**. At present we have no estimate of the magnitude of these displacements which must play an important role in the consideration of local strain. For the relatively low-angle ($\theta_{\mathrm{Cu}\ K\alpha} < 25{\cdot}6°$) diffraction data that are currently available the diffraction patterns can, at least qualitatively, be accounted for by concentration modulations alone. To obtain more information concerning displacement modulations a detailed quantitative analysis of the diffuse scattering data is required, preferably at higher diffraction angles. Further work along these lines is planned. It is interesting to note, however, that even in this low-angle range, diffraction patterns recorded at room temperature are rather smeared in detail compared to the ones shown in Fig. 2 which were recorded at low temperature (120 K), particularly at the higher diffraction angles. Since the orientation disorder is 'locked-in' at growth, these changes must be due to the reduction of thermal displacements and this suggests that any residual *static* displacements must be relatively small by comparison.

7. Concluding remarks

In this paper we have discussed the origins of the unusual diffraction phenomenon which occurs in 1,3-dibromo-2,5-diethyl-4,6-dimethylbenzene. A distinct 'hole' is observed in the disorder diffuse scatting distribution at wavevectors close to $\mathbf{q} = 0$. This is particularly noticeable around the space-group-forbidden (010) Bragg reflection position, but can also be observed at other reciprocal lattice positions.

The diffuse intensity distribution can be described in terms of concentration waves, and we have shown that two different types of mode are possible, a Σ_1 mode which tends to preserve a 2_1-screw axis relationship between neighbouring molecules and a Σ_2 mode which tends to preserve a *c*-glide plane relationship. We have shown that the diffuse scattering is

practically completely explained in terms of modulations of the average structure which are of the Σ_2 symmetry, even though the *average* crystal structure corresponds to a frozen-in Σ_1 modulation.

We argue that the short-range order, which tends locally to preserve the *c*-glide plane, is due to dipole–dipole interactions between molecules. On the other hand, the stability of the lattice over a long range (corresponding to wavevectors close to $\mathbf{q} = 0$) is governed by the short-range repulsive interactions and the ability of the molecules to form a closely packed structure in three different crystallographic planes. In agreement with the general conclusions of Kitaigorodsky (1973) the BEMB2 molecules are more easily able to do this in the space group $P2_1$ than in *Pc*. The 'hole' represents a range of wavevectors for which the strain from the packing forces, as a result of the local breaking of the $P2_1$ symmetry, outweighs the energy gained from the short-range ordering of the molecular dipoles.

References

BRADLEY, C. J. & CRACKNELL, A. P. (1972). *The Mathematical Theory of Symmetry in Solids*. Oxford: Clarendon Press.

CENEDESE, P., BLEY, F. & LEFEBVRE, S. (1984). *Acta Cryst.* A**40**, 228–240.

EPSTEIN, J. & WELBERRY, T. R. (1983). *Acta Cryst.* A**39**, 882–892.

EPSTEIN, J., WELBERRY, T. R. & JONES, R. D. G. (1982). *Acta Cryst.* A**38**, 611–618.

FONTAINE, D. DE (1972). *J. Phys. Chem. Solids*, **33**, 297–310.

FONTAINE, D. DE (1973). *J. Phys. Chem. Solids*, **34**, 1285–1304.

HARBURN, G. H., MILLER, J. S. & WELBERRY, T. R. (1974). *J. Appl. Cryst.* **7**, 36–38.

HARBURN, G. H., TAYLOR, C. A. & WELBERRY, T. R. (1975). *An Atlas of Optical Transforms*. London: Bell.

HAWAKAWA, M., BARDHAN, P. & COHEN, J. B. (1975). *J. Appl. Cryst.* **8**, 87–95.

HUA, G.-L., WELBERRY, T. R. & WITHERS, R. L. (1988). *J. Phys. C*, **21**, 3863–3876.

HUA, G.-L., WELBERRY, T. R. & WITHERS, R. L. (1989). *J. Appl. Cryst.* **22**, 87–95.

KITAIGORODSKY, A. I. (1973). *Molecular Crystals and Molecules*. New York: Academic Press.

LIPSON, H. (1973). *Optical Transforms*. New York: Academic Press.

MCCONNELL, J. D. C. & HEINE, V. (1985). *Phys. Rev. B*, **31**, 6140–6142.

METROPOLIS, N., ROSENBLUTH, A. W., ROSENBLUTH, M. N., TELLER, A. H. & TELLER, E. (1953). *J. Chem. Phys.* **21**, 1087–1092.

TOMAN, K. & FRUEH, A. J. (1976). *Acta Cryst.* B**32**, 521–525.

WEAST, R. C. (1988). Editor. *CRC Handbook of Chemistry and Physics*, 68th ed. Boca Raton, Florida: CRC Press.

WELBERRY, T. R. (1982). *Acta Cryst.* B**38**, 1921–1927.

WELBERRY, T. R. (1986). *J. Appl. Cryst.* **19**, 382–389.

WELBERRY, T. R. & JONES, R. D. G. (1980). *J. Appl. Cryst.* **13**, 244–251.

WELBERRY, T. R. & SIRIPITAYANANON, J. (1986). *Acta Cryst.* B**42**, 262–272.

WELBERRY, T. R. & SIRIPITAYANANON, J. (1987). *Acta Cryst.* B**43**, 97–106.

WELBERRY, T. R. & WITHERS, R. L. (1987). *J. Appl. Cryst.* **20**, 280–288.

WELBERRY, T. R. & WITHERS, R. L. (1990). *J. Appl. Cryst.* Submitted.

WELBERRY, T. R. & ZEMB, T. N. (1988). *J. Colloid Interface Sci.* **123**, 413–426.

WITHERS, R. L., THOMPSON, J. G. & HYDE, B. G. (1989). *Acta Cryst.* B**45**, 136–141.

WOOD, R. A., WELBERRY, T. R. & PUZA, M. (1984). *Acta Cryst.* C**40**, 1255–1260.

YAMAMOTO, A. (1982). *Acta Cryst.* B**38**, 1451–1456.

Acta Cryst. (1990). B**46**, 275–283

Crystal Packing of Hydrocarbons. Effects of Molecular Size, Shape and Stoichiometry

BY A. GAVEZZOTTI

Dipartimento di Chimica Fisica ed Elettrochimica e Centro CNR, Università di Milano, Milano, Italy

(*Received* 24 *May* 1989; *accepted* 21 *November* 1989)

Abstract

The packing energy (PE) and packing modes of hydrocarbon crystals are analyzed statistically using the Cambridge Structural Database. The correlation of PE with several indices of molecular size is discussed; only 19% of the existing hydrocarbon crystal structures are for molecules with an odd number of carbon atoms. Radial distribution functions of the intermolecular contacts peak at a distance which is 0·3–0·5 Å longer than the corresponding sum of the commonly used van der Waals radii. Short contact populations are correlated with various types of packing forces. An effective molecular free surface and a molecular self-packing coefficient are defined to describe shape effects; using these indices, better correlations with PE are obtained, and evidence of the possible formation of inclusion compounds emerges. The effects of the carbon-to-hydrogen ratio on packing are investigated, using the observed den-

0108-7681/90/020275-09$03.00